Technical Note

1970-17

H. Berger

A Theory of Multiple Modes in Avalanche Diodes

9 June 1970

Prepared under Electronic Systems Division Contract AF 19(628)-5167 by

Lincoln Laboratory

MASSACHUSETTS INSTITUTE OF TECHNOLOGY

Lexington, Massachusetts

MASSACHUSETTS INSTITUTE OF TECHNOLOGY
LINCOLN LABORATORY

A THEORY OF MULTIPLE MODES IN AVALANCHE DIODES

HENRY BERGER

Group 41

TECHNICAL NOTE 1970-17

9 JUNE 1970

LEXINGTON MASSACHUSETTS

The work reported in this document was performed at Lincoln Laboratory, a center for research operated by Massachusetts Institute of Technology, with the support of the Department of the Air Force under Contract AF 19(628)-5167.

ABSTRACT

This report develops a multidimensional, dynamic analysis of solid state avalanche diodes. Well-established electromagnetic concepts are applied to a widely used model of the diode and reveal a discrete spectrum of new small-signal modes. The approach used enlarges the conventional perspective and has permitted the discovery that at least one of these new modes appears to possess a high power capability (associated with its two-terminal negative resistance) which has been partially realized experimentally. The lowest-order mode contains all the results of prior quasi-static theories on the normal IMPATT mode, plus additional information which is used to delineate the range of validity of the quasi-static results. Formal discrepancies are uncovered between the usual quasi-static, one-dimensional result for diode impedance used in solid state studies and the dynamic multidimensional result for the normal IMPATT mode developed from microwave circuit theory. However, these discrepancies are numerically quite small except in certain narrow frequency bands.

Accepted for the Air Force
Joseph R. Waterman, Lt. Col., USAF
Chief, Lincoln Laboratory Project Office

CONTENTS

A THEORY OF MULTIPLE MODES IN AVALANCHE DIODES

I. INTRODUCTION

This report develops a multidimensional, dynamic, small-signal analysis of solid state avalanche diodes[1] by applying well-established electromagnetic concepts to a widely used avalanche diode model. Prior theories are one-dimensional and quasi-static, and take into account only longitudinal (z) variations of the fields and currents within the semiconductor.[2] The result is a single quasi-static avalanche mode. In the present work radial (r) and z-variations are considered, and the result is the existence of a spectrum of avalanche modes in the semiconductor. The lowest-order mode is a "volume" mode (i.e., a mode in which the fields and currents do not vary significantly throughout any diode cross section) and is just that mode revealed, in part, by one-dimensional theory. The remaining modes are apparently surface-wave modes[3] (i.e., modes in which the field and current amplitudes inside the semiconductor decrease significantly with distance from the diode-air surface), or similar to surface waves. The idealized solid diode configuration with its contacts may be pictured somewhat as a parallel-plate capacitor or a radial waveguide with perfectly conducting walls, each completely filled with a cylinder of semiconductor material. The dimensions of the diode, however, are several orders of magnitude smaller than ordinary capacitors or radial waveguides (see Fig. 1).

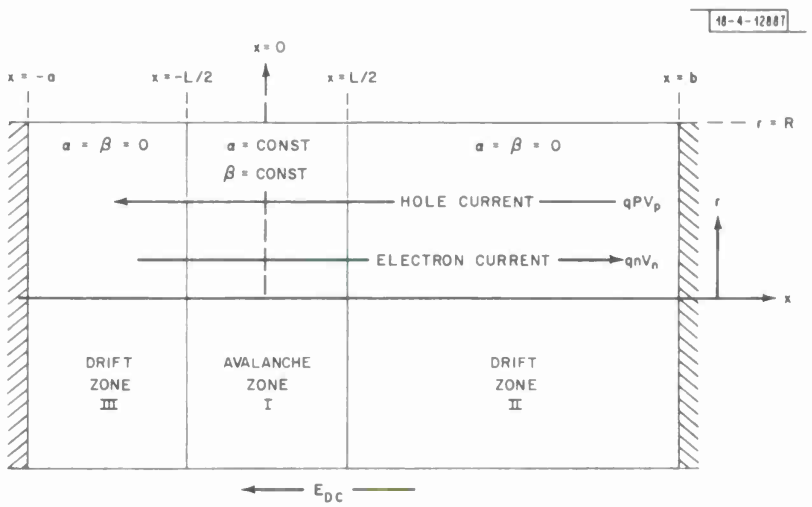

Fig. 1. Multiple uniform layer model of avalanche diode. The crosshatched sections bordering the active regions represent the highly conductive bulk material.

In device work, mode has usually signified a distinctive pattern of device behavior. In this report, avalanche mode is used to signify a self-consistent field and current distribution within the space-charge region of the diode which is consistent with the prevailing boundary conditions at the planar interfaces between the space-charge region and the remaining material of the diode. Each such mode in the preceding sense turns out to be connected with a distinctive pattern of device behavior.

The avalanche modes are obtained by deriving and solving the fundamental small-signal field equation for avalanching carrier interactions with electromagnetic fields. This turns out to be

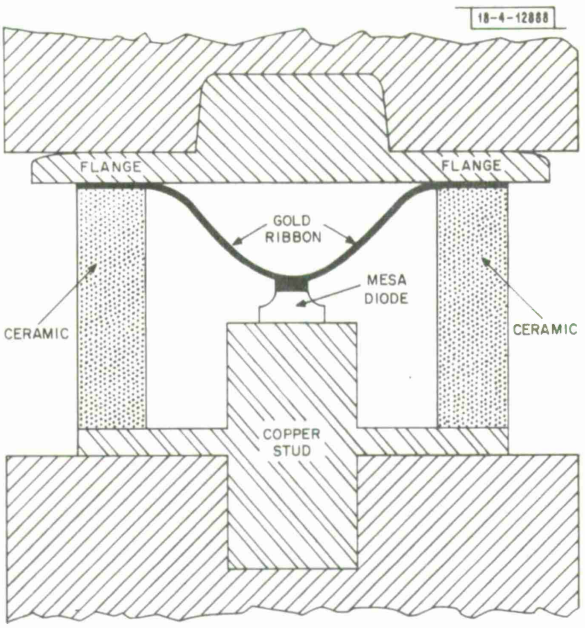

Fig. 2. Simplified model of one type of packaged diode.

a fourth-order wave equation for which the introduction of a spatially and temporally dispersive equivalent conductivity greatly simplifies the method of solution. The avalanche modes within the diode are coupled to the purely electromagnetic modes in the semiconductor package and mount (see Fig. 2). For many package and mount geometries, these modes can be approximated by a TEM radial waveguide mode, with all higher-order radial waveguide modes cut off.[4] The modes in the package and mount are, in turn, coupled to the normal electromagnetic modes of the waveguide or transmission line containing the packaged diode.

The approach used in the present report[5] enlarges the conventional perspective on solid state avalanche diodes in a manner which permits rigorous consideration of complex circumstances which are not directly accessible through present one-dimensional theory. From this perspective one may investigate the influence on avalanche diode operation of:

(a) Higher-order avalanche modes (which apparently possess high power generation capability at microwave frequencies),

(b) Noncircular diode cross sections,

(c) Doughnut or ring shapes[6] (which are used to reduce the diode's thermal resistance),

(d) Nonuniform radial temperature and as well as current profiles induced by thermal effects,[7]

as well as

(e) Determine the diode-package-mount interaction taking into account the cut-off higher-order radial waveguide modes,

(f) Delineate the range of validity of the conventional one-dimensional, quasi-static theory of the normal IMPATT mode, and

(g) Analyze potentially self-resonant IMPATT diodes (which are analogous to self-resonant LSA diodes[8]).

The higher-order avalanche modes appear for the most part to be similar to surface waves and are referred to as SWIMPATT (for surface-wave IMPATT) modes, and are discussed at length elsewhere.[9] The modes are ordered, as is the case of waveguide theory, from smallest

(lowest-order) wavenumber to larger (higher-order) wavenumbers. The SWIMPATT modes are basically a two-dimensional avalanche phenomena.† They are somewhat analogous to the recently discovered two-dimensional wave effects in Gunn-effect diodes.[11-13] The analogy is imperfect, however, because (1) the above-mentioned Gunn-effect diodes are presently designed in the coplanar (or sheet diode) configuration, while the avalanche diodes under discussion are assumed to be in the sandwich configuration described at the beginning of this section, and (2) the Gunn-effect diodes are believed to operate in their lowest-order mode while SWIMPATT are higher-order modes. The present report will develop the fundamental theory. Topics (b), (c), (e), and (g) will be discussed in Ref. 14 as an application of the theory developed here. Topics (a) and (d) will be developed in Refs. 9 and 15. The present report will consider topic (f) and, in outline form, topic (a).

II. MODEL AND BASIC EQUATIONS

The space-charge region of the avalanche diode is modeled as multiple, uniform, tandem layers[1,16] (shown in Fig. 1) within which α_n, the electron ionization rate (which is assumed for simplicity equal to α_p, the hole ionization rate) is assumed to be independent of the longitudinal position z. It is also assumed that the material properties, the DC electric field $\bar{E}_o$, and the DC electron and hole longitudinal currents, J_{no} and J_{po}, are independent of the transverse coordinates within the diode. The space-charge region is assumed to be terminated on both sides by highly conductive material.

In the avalanche zone, $\alpha \equiv \alpha_n = \alpha_p$ is a non-zero quantity, while the drift zones are modeled with $\alpha = 0$ (see Fig. 1). The electron and hole velocities, $\bar{v}_n = v_n \hat{z}_o$ and $\bar{v}_p = -v_p \hat{z}_p$, are taken to be their scattering-limited values (where v_p and v_n are positive constants, and $\hat{z}_o$ is a unit vector in the positive z-direction). Although $v_n \neq v_p$, and $\alpha_n \neq \alpha_p$ in Si and Ge diodes, it is assumed for simplicity[1,16] that $v_n = v_p = v$, and $\alpha_n = \alpha_p = \alpha$ (which holds for GaAs diodes).

The continuity equations for the electron and holes are

$$\frac{\partial n}{\partial t} = \frac{1}{q} \bar{\nabla} \cdot \bar{J}_n + g \tag{1}$$

$$\frac{\partial p}{\partial t} = \frac{-1}{q} \bar{\nabla} \cdot \bar{J}_p + g \tag{2}$$

where $g = \alpha v (n + p)$ is the generation rate, $\bar{J}_n = -qv_n n\hat{z}_o$ and $\bar{J}_p = -qv_p p\hat{z}_o$ are the electron and hole current densities, q is the electronic charge, and n and p are the electron and hole densities. The effects of ohmic radial currents are considered in Ref. 9.

The small-signal time-harmonic approximation for the electric field is

$$\bar{e} = \bar{E}_o + \bar{E}\, e^{j\omega t} \tag{3}$$

where $\bar{E}_o = E_o \hat{z}_o$ is the DC component of $\bar{e}$, $\bar{E}$ is the RF component of $\bar{e}$ with a frequency ω radians per second, and $|\bar{E}_o| >> |\bar{E}|$. A similar description applies to the electron density $N = n_o + n\, e^{j\omega t}$, and the hole density $P = p_o + p\, e^{j\omega t}$. The ionization rate is approximated by the truncated Taylor series

$$\alpha(e) \cong \alpha_o + \alpha'_o E_z \tag{4}$$

---

† This differs from the multidimensional avalanche phenomena in spherical diodes which have recently been discussed.[10]

expanded about E_o with $E_z \equiv \overline{E} \cdot \hat{z}_o$, and α_o, $\alpha_o' \equiv d\alpha/de$, evaluated at $e = E_o$. Equations (1) and (2) may then be used to obtain the continuity equations for the RF carrier densities

$$D_n n - \alpha_o v_p - cE_z = 0 \tag{5}$$

$$D_p p - \alpha_o v_n - cE_z = 0 \tag{6}$$

where only first-order RF terms are retained, $c \equiv -\alpha_o'(J_{no} + J_{po})/q$, and

$$D_n \equiv \frac{\partial}{\partial t} + v \frac{\partial}{\partial z} - \alpha_o v \tag{7}$$

$$D_p \equiv \frac{\partial}{\partial t} - v \frac{\partial}{\partial z} - \alpha_o v \tag{8}$$

In the one-dimensional problem, it is sufficient to add Poisson's equation

$$\overline{\nabla} \cdot \overline{E} = \frac{\partial E_z}{\partial z} = \frac{q}{\epsilon}(p - n) \tag{9}$$

to obtain a complete system of three equations in three unknowns n, p, and E_z. In the multi-dimensional problem, this system is not complete because of the existence of additional field components. In general, this requires the full Maxwell field equations, which are[17]

$$\nabla \times \overline{E} = -\mu_o \frac{\partial \overline{H}}{\partial t} \tag{10}$$

$$\nabla \times \overline{H} = \overline{J}_n + \overline{J}_p + \epsilon \frac{\partial \overline{E}}{\partial t} \tag{11}$$

where the constitutive relations $\overline{D} = \epsilon \overline{E}$ and $\overline{B} = \mu_o \overline{H}$ have already been used. Equations (5), (6), (10), and (11) constitute a complete set of equations. Equations (5) and (6) may be combined to give

$$[D_n D_p - (\alpha_o v)^2]\, n = c\,[D_p + \alpha_o v]\, E_z \tag{12}$$

$$[D_n D_p - (\alpha_o v)^2]\, p = c\,[D_n + \alpha_o v]\, E_z \tag{13}$$

Multiplying Eqs. (12) and (13) by $-qv$, and summing

$$[D_n D_p - (\alpha_o v)^2]\,[J_n + J_p] = 2\alpha_o' J_o v \frac{\partial E_z}{\partial t} \tag{14}$$

is obtained.

Equations (10) and (11) can be combined to obtain

$$\overline{\nabla} \times \overline{\nabla} \times \overline{E} = -\mu_o \frac{\partial}{\partial t}(\overline{J}_n + \overline{J}_p) - \mu_o \epsilon \frac{\partial^2 \overline{E}}{\partial t^2} \tag{15}$$

Operating on Eq. (15) by the operator $D_n D_p - \alpha_o^2 v^2$ to eliminate J_n and J_p, it follows that

$$[D_n D_p - (\alpha_o v)^2]\, \overline{\nabla} \times \overline{\nabla} \times \overline{E} = -2\mu_o \alpha_o' J_o v \frac{\partial^2 E_z}{\partial t^2} \hat{z}_o - \epsilon \mu_o [D_n D_p - (\alpha_o v)^2] \frac{\partial^2 \overline{E}}{\partial t^2} \tag{16}$$

Equation (16) is the fundamental wave equation for the avalanche diode model considered in this report. Generalizations to the important case of ohmic and diffusive radial currents are considered in Ref. 9. Equation (16) is a fourth-order partial differential equation and, in general,

difficult to solve directly. For the circumstances being considered, it is useful to take advantage of the fact that the D_n and D_p operators are constant coefficient and commute with the operator $(\overline{\nabla} \times \overline{\nabla} \times)$. Consider electric fields which are describable by

$$\overline{E} = \sum_i \overline{E}_i \tag{17}$$

where

$$\overline{E}_i = \overline{\mathcal{E}}_i(r, \varphi)\, e^{j(\omega t - K_i z)} \tag{18}$$

then

$$[D_n D_p - (\alpha_o v)^2]\, \overline{E}_i = F_i(\omega, K_i)\, \overline{E}_i \tag{19}$$

where $F_i(\omega, K_i) \equiv [j(\omega - vk_i) - \alpha_o v]\,[j(\omega + vK_i) - \alpha_o v]$. Using the above results, along with $\partial/\partial t = j\omega$, Eq. (16) becomes

$$\overline{\nabla} \times \overline{\nabla} \times \overline{E}_i = \omega^2 \mu_o \overline{\overline{\epsilon}}_i \cdot \overline{E}_i \tag{20}$$

where the equivalent permittivity matrix ϵ_i is defined by

$$\overline{\overline{\epsilon}}_i = \begin{bmatrix} \epsilon\left[1 + \dfrac{\sigma_i}{j\omega\epsilon}\right] & 0 & 0 \\ 0 & \epsilon & 0 \\ 0 & 0 & \epsilon \end{bmatrix} \tag{21}$$

in which ϵ is the standard dielectric permittivity of the material and σ_i is the equivalent conductivity defined by

$$\sigma_i \equiv \frac{-2j\omega v \alpha_o' J_o}{\omega^2 + 2j\omega\alpha_o v - (K_i v)^2} \tag{22}$$

with $J_o = J_{no} + J_{po}$. σ_i is the conductivity in the sense that it can be shown from Eq. (14) that

$$J_{ni} + J_{pi} = \sigma_i E_{zi} \tag{23}$$

Equation (20) may be written directly in terms of an equivalent conductivity matrix $\overline{\overline{\sigma}}_i$ as

$$\overline{\nabla} \times \overline{\nabla} \times \overline{E}_i = -j\omega\mu_o [\overline{\overline{\sigma}}_i + j\omega\epsilon \overline{\overline{1}}] \cdot \overline{E}_i \tag{24}$$

where $\overline{\overline{1}}$ is the unity matrix and

$$\overline{\overline{\sigma}}_i = \begin{bmatrix} \sigma_i & 0 & 0 \\ 0 & 0 & 0 \\ 0 & 0 & 0 \end{bmatrix} \tag{25}$$

The influence of highly conductive regions sandwiching the space-charge region is approximated by using the boundary conditions appropriate to infinitely conductive material, i.e., the radial component of E is zero at $z = \pm L/2$. The fields are expressible in terms of TE and TM cylindrical wave modes which are similar in some respects to the TE and TM radial waveguide modes.[17] In addition, the TE radial wave modes are uncoupled to the avalanche currents and, hence, are the same as for a "cold" dielectric cylinder bounded by metal caps. Thus, only TM radial wave modes ($H_z = 0$) will be considered. In Ref. 14, the effect of variations of the fields and currents with azimuthal angle is considered in connection with the influence of noncircular diode cross section.

The TM radial wave avalanche modes have non-zero field components E_z, H_φ, and E_r (when there are no azimuthal variations) and are also similar in many respects to the well-known small-signal TM modes in an axially directed electron beam of finite radius.[18] When a TM radial wave avalanche mode has "sufficiently small" radial variations (and no azimuthal variations), then the radial electric field component E_r will be shown in a later section to have a negligible magnitude from the point of view used in most computations. The resulting avalanche mode can be envisioned to be essentially a TEM (in the r-direction) wave with only E_z and H_φ as significant non-zero field components. This quasi-TEM mode for which the z-variations are derivable from one-dimensional theory (which conventionally explicitly discusses only the E_z field component) is the normal IMPATT mode. The H_φ field component for the normal IMPATT mode is readily derivable in the terms of the z-component of the total current density $J_T = J_n + J_p + j\omega E_z$ which is shown in Sec. V to be essential independent of r and z (as is already widely known).† The TEM radial wave avalanche mode differs most significantly in mathematical form from the TEM radial waveguide mode[17] (which has E_z and H_φ as the only non-zero field components) by virtue of the z-variations in E_z which the space-charge waves in the avalanche diode produce. The H_φ field component is independent of z in both the TEM avalanche mode and the TEM radial waveguide mode. By contrast, it may be noted that the quasi-TEM radial wave mode (with negligible value for E_r) in an axially directed electron beam of "large" finite radius does exhibit z-variations in E_z (Ref. 18).

Solution of the associated boundary value problem, posed below, yields a discrete spectrum of modes within the diode, each of which has particular field and current distributions (which vary with frequency) within the diode. The relative amplitudes of the modes would be determined by imposing boundary conditions at the "rim" of the semiconducting pill, i.e., at r = R, in the same manner as is done for radial waveguides to reflect the diode-circuit interaction.

III. AVALANCHE ZONE

From the basic equation, Eq. (24), it follows without further assumptions that TM waves of the form $\mathcal{E}_{zi}(r)\, e^{j(\omega t - k_i z)}$ must satisfy

---

† Using Ampere's rule in the form

$$\int_0^{2\pi} H_\varphi R d_\varphi = \int_0^{2\pi} \int_0^R J_T r d\varphi\, dr$$

one obtains $H_\varphi = rJ_T/2$ inside the diode and $R^2 J_T/2r$ outside the diode (but nearby), where R is the diode radius.

$$\frac{1}{r}\frac{\partial}{\partial r}\left(r\frac{\partial \mathcal{E}_z}{\partial r}\right) + T_a^2 \mathcal{E}_z = 0 \tag{26}$$

where the subscript i has been dropped from $\mathcal{E}_z$ for simplicity. Note that the identity $\overline{\nabla} \times \overline{\nabla} \times \overline{E} = \overline{\nabla}(\overline{\nabla} \cdot \overline{E}) - \nabla^2 \overline{E}$ is not required in obtaining Eq. (26), and further does not reduce the algebraic complexity since $\overline{\nabla} \cdot \overline{E} \neq 0$. The remaining symbols are defined by

$$T_a^2 \equiv \frac{(K_o^2 - K_i^2)(K_m^2 - K_i^2)}{(K_m^2 + K_a^2 - K_i^2)} \tag{27}$$

$$K_o^2 \equiv \omega^2 \mu_o \epsilon \tag{28}$$

$$K_m^2 \equiv (\omega/v)^2 + 2j\alpha_o(\omega/v) - K_a^2 \tag{29}$$

$$K_a^2 \equiv (\omega_a/v)^2 \quad , \quad \omega_a^2 = 2\alpha_o' J_o v/\epsilon \quad , \tag{30}$$

K_o is the standard dielectric wavenumber, $\pm K_m$ are the wavenumbers calculated by Misawa[16] (along with zero) for one-dimensional space-charge waves in avalanching carrier streams, and ω_a is the avalanche frequency originally derived by Gilden and Hines[19] below which the equivalent diode conductance is positive in their theory.

Equation (27) can be rewritten as

$$K_i^4 - K_i^2(K_m^2 + K_o^2 - T_a^2) + [K_o^2 K_m^2 - T_a^2(K_m^2 + K_a^2)] = 0 \tag{31}$$

from which it is clear that there are four values of K_i corresponding to T, with

$$K_{i1} = -K_{i2} \quad , \quad K_{i3} = -K_{i4} \tag{32}$$

For simplicity the first subscript, i, of the K's in Eq. (32) will be dropped. Thus, the only non-singular solution that includes r = 0 is†

$$E_x = J_o(T_a r) \sum_{i=1}^{4} A_i e^{-jK_i z} \tag{33}$$

where $J_o(Tr)$ is the zeroth order Bessel function of the first kind, A_i are constants, and the $e^{j\omega t}$ dependence is understood. From Eqs. (10) and (33), it follows that

$$H_\varphi = j\omega\epsilon T_a J_1(T_a r) \sum_{i=1}^{4} \left(\frac{A_i e^{-jK_i z}}{K_o^2 - K_i^2}\right) \tag{34}$$

and

$$E_r = jT_a J_1(T_a r) \sum_{i=1}^{4} \left(\frac{K_i A_i e^{-jK_i z}}{K_o^2 - K_i^2}\right) \tag{35}$$

where $J_1(Tr)$ is the first-order Bessel function of the first kind. Equations (33) to (35) describe the only non-zero field components.

† Ring (or doughnut) diodes require both Bessel functions of the first and second kind for a complete description.

Equations (12) and (13) can be used to obtain

$$J_n = J_o(T_a r) \sum_{i=1}^{4} \sigma_{ni} A_i e^{-jK_i z} \tag{36}$$

$$J_p = J_o(T_a r) \sum_{i=1}^{4} \sigma_{pi} A_i e^{-jK_i z} \tag{37}$$

where $\sigma_{ni} = (\sigma_i/2)\,(1 + vK_i/\omega)$, and $\sigma_{pi} = (\sigma_i/2)\,(1 - vK_i/\omega)$. Note $\sigma_{ni} + \sigma_{pi} = \sigma_i$. The customary boundary conditions (these are not altered by the presence of drift zones) which are

$$J_n = 0 \quad \text{at} \quad z = -\frac{L}{2} \tag{38}$$

$$J_p = 0 \quad \text{at} \quad z = +\frac{L}{2} \tag{39}$$

are symmetric so that when the drift zones are symmetric about $z = 0$

$$J_n(z) = J_p(-z) \tag{40}$$

It follows from this symmetry that

$$A_1 = A_2 \quad , \quad A_3 = A_4 \tag{41}$$

Equations (33) to (35) then simplify to

$$E_x = J_o(T_a r)\, 2A_1 \left[\cos(K_1 z) + M \cos(K_3 z)\right] \tag{42}$$

$$H_\varphi = 2j\omega\epsilon\, T_a A_1 J_1(T_a r) \left[\frac{\cos(K_1 z)}{K_o^2 - K_1^2} + \frac{M \cos(K_3 z)}{K_o^2 - K_3^2}\right] \tag{43}$$

$$E_r = 2jT_a A_1 J_1(T_a r) \left[\frac{K_1 \sin(K_1 z)}{K_o^2 - K_1^2} + \frac{MK_3 \sin(K_3 z)}{K_o^2 - K_3^2}\right] \tag{44}$$

where

$$M \equiv \frac{A_3}{A_1} = -\left[\frac{\omega \cos\Theta_1 + jvK_1 \sin\Theta_1}{\omega \cos\Theta_3 + jvK_3 \sin\Theta_3}\right]\left[\frac{\omega^2 - (vK_3)^2 + 2j\omega V\alpha_o}{\omega^2 - (vK_1)^2 + 2j\omega V\alpha_o}\right] \tag{45}$$

with $\Theta_1 = k_1 L/2$, and $\Theta_3 = K_3 L/2$. In the absence of symmetry, the results are more complex.

IV. DRIFT ZONE

When α and α' are almost but not exactly equal to zero, Eqs. (5) and (6) apply in the same form as for the avalanche zone. Thus, the results for the drift zone are

$$E_x = J_o(T_d r) \sum_{i=1}^{4} G_i e^{-j\beta_i z} \tag{46}$$

$$H_\varphi = j\omega\epsilon\, T_d J_1(T_d r) \sum_{i=1}^{4} \left(\frac{G_i}{K_o^2 - \beta_i^2} \right) e^{-j\beta_i z} \tag{47}$$

$$E_r = jT_d J_1(T_d r) \sum_{i=1}^{4} \left(\frac{\beta_i G_i}{K_o^2 - \beta_i^2} \right) e^{-j\beta_i z} \tag{48}$$

where $\beta_1 = -\beta_2$, $\beta_3 = -\beta_4$ and G_i are constant amplitudes. However, there is not the same symmetry as in the drift region, so $G_1 \neq G_2$ and $G_3 \neq G_4$. The equation for T^2 remains in the same form, i.e.

$$T_d^2 = \frac{(K_o^2 - \beta_i^2)(K_m^2 - \beta_i^2)}{(K_m^2 + K_a^2 - \beta_i^2)} \tag{49}$$

But now

$$K_a^2 \to \Delta_a \to 0 \quad , \qquad \text{because } \alpha_o' \to 0$$

$$K_m^2 \to \beta^2 + \Delta_m,\ \Delta_m \to 0 \quad , \qquad \text{because } \alpha_o,\ \alpha_o' \to 0$$

where $\beta = w/v$ and Δ_a and Δ_m are K_a^2 and $K_m^2 - \beta^2$ evaluated at arbitrarily small but not zero values of α_o and α_o'.

Thus, Eq. (49) reduces to

$$T_d^2 = \frac{(K_o^2 - \beta_i^2)(\beta^2 - \beta_i^2 + \Delta_m)}{\beta^2 - \beta_i^2 + \Delta_m + \Delta_a} \tag{50}$$

Equation (50) can be rewritten in the form

$$[\beta_i]^4 - [\beta_i]^2 (\beta^2 + K_o^2 - T_d^2) + \beta^2 (K_o^2 - T_d^2) = 0 \tag{51}$$

where Δ_a and Δ_m have been taken as zero for simplicity. Continuity of fields at $x = \pm L/2$ requires that $T_a = T_d$. The solutions to Eq. (51) are then

$$\beta_i = \pm\beta,\ \pm\sqrt{K_o^2 - T_a^2} \qquad (i = 1, 2, 3, 4) \tag{52}$$

The above description of the drift zone is not so complex as that required for the avalanche zone. For the unsymmetric case, there are four unknown coefficients (the G_i's) for each of two drift zones, plus four unknown coefficients (the A_i's) for the avalanche zone totaling twelve unknown coefficients. There are twelve boundary conditions that must be satisfied at the various interfaces. They are $E_r = J_p = 0$ at $x = b$, $E_r = J_n = 0$ at $x = -a$, and continuity of E_r, H_φ, J_n, and J_p at $z = \pm L/2$. This information is necessary and sufficient for the determination of the ratios of eleven of the coefficients to the twelfth, plus the radial wavenumber T_a. Once T_a is determined, then the longitudinal wavenumbers K_i and β_i can be calculated.

In the special case when $K^2 - T_a^2 = \beta^2$ (which corresponds to surface waves because here $|T_a|\, R > 1$ typically), we see from Eq. (52) that a degenerate situation occurs in which case eigenfunctions $A_i\, e^{-j\beta_i z}$ are no longer valid. To analyze this special case, one must then return to

the fundamental avalanche equation, Eq. (16), and rederive its solutions anew. An alternative approach is to analyze the drift zone degenerate case with $\alpha_o = \alpha_o' = 0$ to begin with, as opposed to calculating the solutions from the avalanche zone results by letting α_o, $\alpha_o' \to 0$ as we have done here. However, no further insight is gained from such an approach. The basic wave properties of the nondegenerate surface modes are outlined in Refs. 3 and 9.

V. THE QUASI-TEM RADIAL WAVE MODE (NORMAL IMPATT)

In this section it is demonstrated that, when $|T_a|\, r \ll 1$ for $0 < r \leqslant R$, the preceding TM waves reduce to a quasi-TEM cylindrical bulk wave for which the axial component of electric field is that derived by quasi-static, one-dimensional theory for the normal IMPATT mode.

The first part of this demonstration consists of deriving approximate expressions for the K_i's. This is accomplished by solving Eq. (25), for K_i in terms of T_a, with the assumption that $|T_a|^2 \ll |K_m|^2$. For typical parameter values of an avalanche diode operating at microwave frequencies $(K_a/K_m)^2$ is of order unity so that $|T_a|^2\, |1 + (K_a/K_m)^2| \ll |K_m|^2$ and $K_o^2 \ll |K_m|^2$. The solutions to Eq. (31) are then

$$K_1^2 = K_2^2 \simeq K_o^2 - T_a^2\,[1 + (K_a/K_m)^2] \tag{53}$$

$$K_3^2 = K_4^2 \simeq K_m^2 - K_o^2 + T_a^2\,[1 + (K_a/K_m)^2] \tag{54}$$

Note from the above that $K_1^2 + K_3^2 = K_m^2$. The longitudinal length of the space-charge region is of the order of 10 μm or, typically, much less. Thus $\cos(K_1 z) \simeq 1$, $\sin(K_1 z) \simeq K_1 z$. In addition the assumption $|T_a|\, r \ll 1$ leads to $J_o(T_a r) \simeq 1$, $J_1(T_a r) \simeq T_a r/2$. Then Eqs. (42) through (44) reduce to

$$E_z \simeq 2A_1\,[1 + M_m \cos(K_m z)] \tag{55}$$

$$H_\varphi \simeq A_1 \left\{ \frac{j\omega\epsilon r}{1 + (K_a/K_m)^2} + \left(\frac{T_a}{K_m}\right)^2 [j\omega\epsilon r M_m \cos(K_m z)] \right\}$$

$$\simeq A_1(\sigma_o + j\omega\epsilon)\, r \tag{56}$$

$$E_r \simeq -jA_3 \sin(K_m z)\, M_m \left(\frac{T_a}{K_m}\right) (T_a r) \tag{57}$$

σ_o represents σ_i with $K_i = 0$. E_z is now in the TEM form, and H_φ is in the TEM form except for a correction term which is negligible for $|T_a/K_m| \ll 1$. E_r is effectively zero because it is negligible for $|T_a/K_m| \ll 1$, $|T_a|\, r \ll 1$.

Equation (45) reduces to

$$M_m \equiv \frac{A_3}{A_1} = \frac{\sigma_o}{\epsilon(j\omega \cos\Theta_m - VK_m \sin\Theta_m)} \tag{58}$$

where $\Theta_m = K_m L/2$.

The total current in the z-direction, $J_T = j\omega\epsilon E_z + J_n + J_p$, can be obtained from Eqs. (36), (37), and (42). The result is

$$J_T = 2A_1 J_o(T_a r)\,[(\sigma_1 + j\omega\epsilon)\cos(K_1 z) + M_m(\sigma_3 + j\omega\epsilon)\cos(K_3 z)] \tag{59}$$

where $\sigma_1 = \sigma_i$ when i = 1, and $\sigma_3 = \sigma_i$ when i = 3. When Eqs. (53) and (54) hold, then $\sigma_1 \simeq \sigma_o$, and $\sigma_3 \simeq -j\omega\epsilon$. Thus, when $|T_a|\, r \ll 1$, then

$$J_T \simeq 2A_1(\sigma_o + j\omega\epsilon) \tag{60}$$

Observe that, although J_T is independent of position, it is a function of frequency, ionization rate, saturated carrier velocity, and the DC current density.

If one attempts to approximate the preceding quasi-TEM radial wave by a cylindrical wave which is TEM without approximation, i.e., where $E_z \neq 0$, and $H_\varphi \neq 0$ but $E_r \equiv 0$ (which is not possible because the boundary conditions could not be satisfied), then a somewhat unlikely result is obtained. It can be shown that[20] for the exact TEM radial wave the unity term in the R.H.S. of Eq. (55) is associated with T_a given by

$$T_a^2 = T_o^2 \equiv -j\omega\mu_o(\sigma_o + j\omega\epsilon) = K_o^2 - j\omega\mu_o\sigma_o \tag{61}$$

while $T_a \equiv 0$ for the remaining cosine term, i.e.,

$$E_z \simeq 2A_1\,[J_o(T_o r) + M_m \cos(K_m z)] \tag{62}$$

Inasmuch as σ_o plays the role, in several instances, of somewhat of an effective over-all conductivity (independent of K_i) for the quasi-TEM (normal IMPATT) mode, it appears plausible to take T_a^2 as given by Eq. (61). Then Eq. (55) could be written more descriptively as

$$E_z = 2A_1 J_o(T_o r)\,[1 + M_m \cos(K_m z)]$$

Several important properties of T_o are readily determined.

(a) If $\omega \gg \omega_a$ (and typically $\omega_a \geqslant 2\alpha_o v$),

then $T_o^2 \approx K_o^2$ = real.

(b) If $\omega \to 0$,

then $T_o \to \left(\frac{K_o\omega_a}{2j\omega\alpha_o v}\right)(1 + j) = (1 - j)\left(\frac{K_o}{2\alpha_o v}\right)\sqrt{\frac{\mu_o\epsilon}{\omega}}$

(c) If $\omega = \sqrt{\omega_a^2 + (2\alpha_o v)^2}$,

then $\mathrm{Re}(T_o^2) = 0$.

The quasi-TEM radial wave mode within the IMPATT diode, as explicitly displayed by Eqs. (55), (56), and (57) can be now readily contrasted with the TEM radial electromagnetic waveguide mode in the diode package and mount which is, in general, described by

$$E_x = 2AJ_o(K_o r) \tag{63}$$

$$H_\varphi = -K_o 2AJ_1(K_o r)/j\omega\mu_o \tag{64}$$

where $K_o^2 = \omega^2\mu_o\epsilon_o$. This reduces to

$$E_x = 2A \tag{65}$$

$$H_\varphi = j\omega\epsilon Ar \tag{66}$$

for the usual case where $K_o r << 1$.

The influence of the IMPATT diode's finite radius on its impedance is determined below to be

$$\frac{Z_c}{Z_o} = \frac{T_a R J_o(T_a R)}{2J_1(T_a R)} \tag{67}$$

where Z_o and Z_c are the impedances derived from the one and multidimensional theories, R is the radius of the diode, and one may use the simple estimate of T_a^2 provided by Eq. (61). The results, shown in Figs. 3 through 10, demonstrate that significant deviations (ranging from 5 to 50 percent or higher) from the quasi-static, one-dimensional results occur only within a 100-MHz band surrounding the threshold frequencies of negative impedance and the reactive resonance frequencies. The substantial deviations illustrated may be easily obscured in practice by dissipative losses in the contacts, package, and mount, as well as the usual tolerances in measurements.

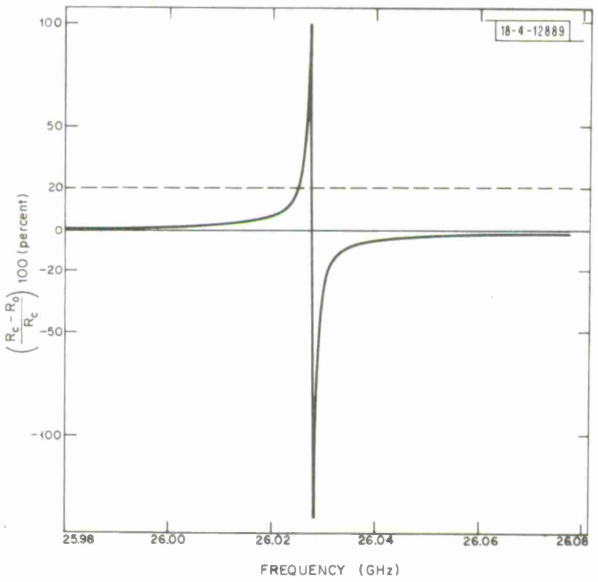

Fig. 3. Relative percentage difference between normal IMPATT resistance (in a 100-MHz band surrounding the negative resistance threshold) as calculated from conventional quasi-static one-dimensional and dynamic multidimensional theories. Parameters are $J_o = 3760$ amp/cm^2, $L = 0.50\,\mu$m, $b - L/2 = 0.92\,\mu$m, and $v = 8.5 \times 10^6$ cm/sec.

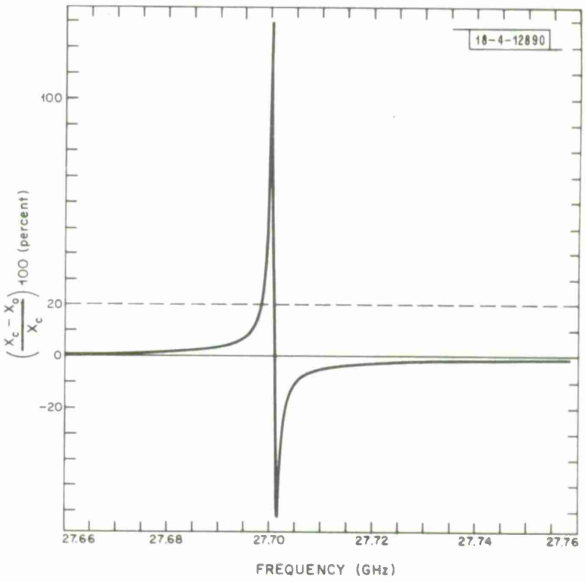

Fig. 4. Relative percentage difference between normal IMPATT reactance (in a 100-MHz frequency band surrounding reactive resonance) as calculated from one-dimensional quasi-static and dynamic multidimensional theories. Parameters same as for Fig. 3.

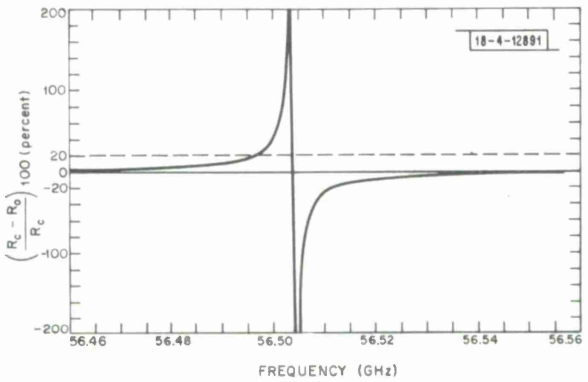

Fig. 5. Same type of plot as in Fig. 3, using parameters J_o = 10,350 amp/cm^2, L = 0.22 μm, b − L/2 = 0.39 μm, and v = 8.5 × 10^6 cm/sec.

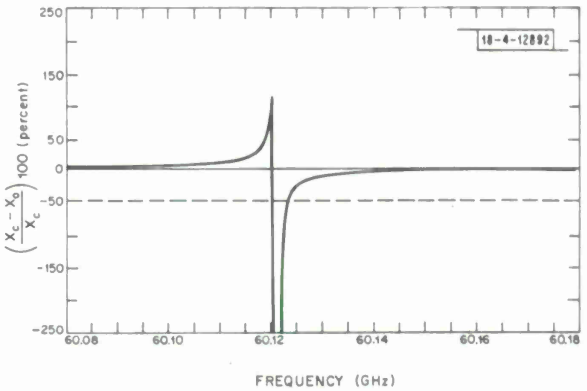

Fig. 6. Same type of plot as in Fig. 4, using same parameters as for Fig. 5.

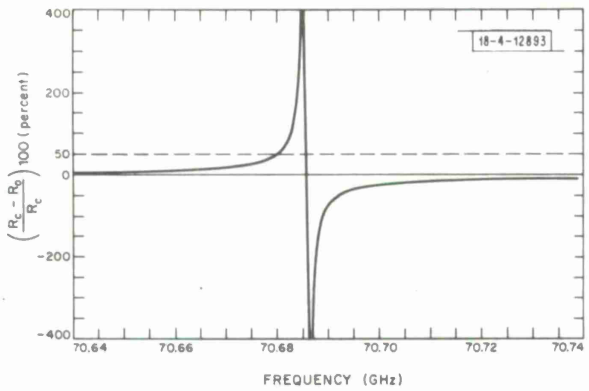

Fig. 7. Same type of plot as in Fig. 3, using parameters J_o = 14,000 amp/cm, L = 0.17 μm, b − L/2 = 0.30 μm, and v = 8.5 × 10^{-6} cm/sec.

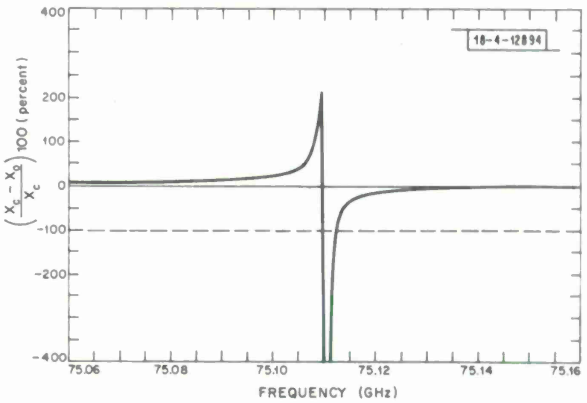

Fig. 8. Same type of plot as in Fig. 4, using same parameters as for Fig. 7.

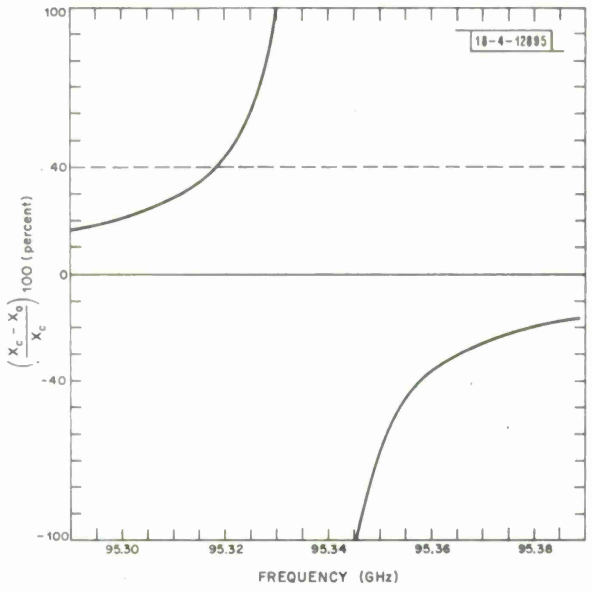

Fig. 9. Same type of plot as in Fig. 3, using parameters $J_o = 23{,}530\ \text{amp/cm}^2$, $L = 0.12\,\mu\text{m}$, $b - L/2 = 0.21\,\mu\text{m}$, and $v = 8.5 \times 10^6\ \text{cm/sec}$.

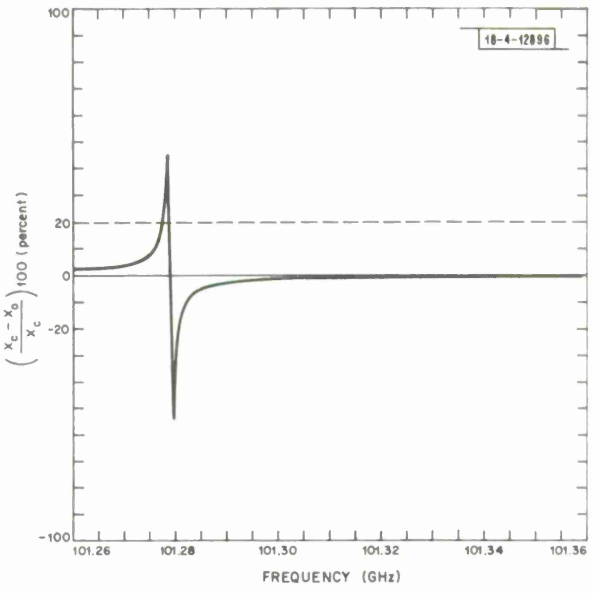

Fig. 10. Same type of plot as in Fig. 4, using same parameters as for Fig. 9.

VI. IMPEDANCE OF THE AVALANCHE REGION

In this section, Eq. (67), which explicitly displays the dependence of the impedance of a diode operating in the normal IMPATT mode on diode radius R, is derived. We find that the usual quasi-static, one-dimensional result for impedance used in diode work, Eq. (71) below, differs numerically over narrow frequency bands from the dynamic, multidimensional result for the same quantity.

For convenience, we repeat here the appropriate equations for the normal IMPATT mode (where $\cos(K_i Z) \simeq 1$, and $K_3 \simeq K_m$) explicitly including the radial dependence. These are, from Eqs. (42), (43), and (44),

$$E_z \simeq 2A_1 J_o(T_a r)\,[1 + M_m \cos(K_m z)] \tag{68}$$

$$H_\varphi \simeq 2A_1 J_1(T_a r)\,(\sigma_o + j\omega\epsilon)/T_a \tag{69}$$

$$E_r \simeq 0 \tag{70}$$

The impedance of a diode operating in a normal IMPATT mode is given in general as

$$Z = \frac{V}{I_t} \tag{71}$$

where I_t is the total current through the diode of radius R and

$$V = \int_{-L/2}^{L/2} E_z dz \tag{72}$$

is the voltage across the diode. The voltage may be written, from Eqs. (68) and (72), as

$$V = J_o(T_a r)\, V_o \tag{73}$$

where

$$V_o = \int_{-L/2}^{L/2} 2A_1 \left[1 + M_m \cos(K_m z)\right] dz \tag{74}$$

is the voltage arising in the conventional one-dimensional theory. It is clear from Eq. (73) that the voltage remains an ambiguous quantity until an appropriate value of r is chosen. The total current is, from Eq. (59),

$$I_t = \iint J_t \, r d\varphi \, dr \tag{75}$$

Eqs. (71), (73), and (75) yield the conventional one-dimensional impedance $Z_o = V_o/\pi R^2(\sigma_o + j\omega\epsilon)$, when $J_o(Tr) \simeq 1$, and J_t is given by Eq. (60).

The impedance of a one-port (two-terminal) is given in microwave circuit theory by[17,20]

$$Z_c = \frac{P_t}{|I|^2} \tag{76}$$

where

$$P_t = \oiint_{A_c} \overline{E} \times \overline{H}^* \cdot d\overline{A} \tag{77}$$

which represents the complex electromagnetic power flow through the enveloping surface A_c (which in the present case is the "exposed" cylindrical surface comprising the diode-air interface at r = R). I in Eq. (76) represents the terminal current which may be chosen as the I_t used in the present report. The total current is related to the magnetic field by Ampere's Law [which is simply the usual integral form of Eq. (11)]

$$I_t = \oint H_\varphi R \, d\varphi \tag{78}$$

where azimuthal symmetry has been assumed, R is the outer radius of the diode and H_φ in Eq. (78) is evaluated at r = R. Since H_φ is independent of φ (for circular cross-section diode), Eq. (78) becomes

$$\begin{aligned} I_t &= 2\pi R H_\varphi \\ &= 4\pi A_1 R J_1(T_a R)\,(\sigma_o + j\omega\epsilon)/T_a \end{aligned} \tag{79}$$

For the normal IMPATT mode, Eq. (77) becomes

$$P_t = \oiint_{A_c} (E_z H_\varphi^*)\, R \, d\varphi \, dz \tag{80}$$

where the integrand of Eq. (80) is evaluated at r = R. This result may be rewritten as

$$\begin{aligned} P_t &= \left(\oint H_\varphi^* R \, d\varphi\right)\left(\int_{-a}^{b} E_z \, dz\right) \\ &= I_t^* V \quad \text{(evaluated at } r = R) \end{aligned} \tag{81}$$

where Eqs. (72) and (78) have been used along with knowledge, from Eqs. (68) and (69), that H_φ is independent of z and E_z is independent of φ. Equation (76) thus leads to

$$Z_c = \frac{J_o(T_a R)\, V_o}{4\pi A_1 R_2 J_1(T_a R_2)\,(\sigma_o + j\omega\epsilon)/T_a} \tag{82}$$

or

$$Z_c = \left(\frac{T_a R J_o(T_a R)}{2J_1(T_a R)}\right) Z_o \qquad \text{[Eq. (67)]}$$

It is not unexpected that a multidimensional, dynamic description of a diode should yield some sort of corrections to the one-dimensional, quasi-static results. Such is the case, for example, for the classical capacitor. However, such a theory also reveals the potential existence of other modes, as mentioned earlier, which can never be obtained from the one-dimensional, quasi-static theory.

VII. THE DRIFT ZONE IN THE QUASI-STATIC APPROXIMATION

In this section the quasi-static one-dimensional description of the drift zone interactions are retrieved from the general theory of Sec. IV.

When $|T|\, r \ll 1$, $0 \leqslant r \leqslant R$

$$J_n = \sum_{i=1}^{4} \sigma_{ni} G_i\, e^{-j\beta_i z} \tag{83}$$

$$J_p = \sum_{i=1}^{4} \sigma_{pi} G_i\, e^{-j\beta_i z} \tag{84}$$

similar to the avalanche zone where β_i replaces K_i in σ_{ni} and σ_{pi}. For

$$\beta_1 = -\beta_2 \simeq T^2 - K_o^2 \rightarrow \text{order of magnitude of } \omega^2 \mu_o \epsilon \tag{85}$$

then $\omega^2 \gg (v\beta_i)^2$ for all ω, so $\sigma_{n1} \simeq \sigma_{n2} \simeq \sigma_{p1} \simeq \sigma_{p3} \simeq \sigma_o$ goes to zero where α_o and α_o' go to zero. Also $\beta_3^2 = \beta_4^2 \simeq 2j(\omega/v)\,\alpha_o - (2\alpha_o' J_o/v\epsilon) + (\omega/v)^2$, hence $\beta_3 = -\beta_4 \simeq \omega/v + j\alpha_o - \alpha_o J_o/\omega\epsilon$ for sufficiently small α_o and α_o'. From this it can be shown that σ_{n4} and σ_{p3} go to zero while σ_{p4} and σ_{n3} go to $-j\omega\epsilon$.

Thus

$$J_n \simeq -j\omega\epsilon G_3\, e^{-j\beta x} \tag{86}$$

$$J_p \simeq -j\omega\epsilon G_4\, e^{+j\beta z} \tag{87}$$

The boundary condition $J_p = 0$, at $z = b$, implies from the above that $G_4 = 0$. For the customary range of values for z, $e^{jK_o z} \simeq 1$ with considerable accuracy. Thus, Eqs. (46), (47), and (48) reduce, for the quasi-TEM case, to

$$E_x \simeq G_o + G_3\, e^{-j\beta z} \tag{88}$$

$$H_\varphi \simeq \frac{j\omega\epsilon r}{2}\left(G_o - G_3\,\frac{T^2}{\beta}\,e^{-j\beta z}\right) \tag{89}$$

$$E_r \simeq \frac{jr}{2}\left[K_o(G_1 - G_2) - G_3\,\frac{T^2}{\beta}\,\beta\,e^{-j\beta z}\right] \tag{90}$$

where $G_o = G_1 + G_2$. The boundary condition $E_r = 0$ at $z = b$ implies that $G_1 = G_2$ for T^2/β sufficiently small, so the above reduces further to $E_x \simeq G_o + G_3\,e^{-j\beta z}$, $H_\varphi \simeq j\omega\epsilon r G_o/2$, and $E_r \simeq 0$. Thus the quasi-static results can be retrieved. The large radius result of Eq. (67) applies equally well to the drift zone.

VIII. CONCLUSIONS

This report has presented a multidimensional analysis of avalanche diodes which exposes the existence of new modes (TM cylindrical waves) in the semiconductor in addition to that obtained through prior one-dimensional theories.[1,16] The main parameters characterizing the radial variation of fields and currents are (1) the frequency, (2) the avalanche frequency, as defined by Gilden and Hines,[19] and (3) the wavenumbers for one-dimensional space-charge waves on avalanching carriers as determined by Misawa.[16] Associated with each mode are four plane waves traveling along the longitudinal axis of the semiconductor. The results obtained from one-dimensional quasi-static analysis turn out to be contained in a quasi-TEM cylindrical "volume" wave which is retrieved from the lowest-order mode of the multidimensional avalanche mode spectrum. The total current for the quasi-TEM mode, which in prior analyses is an unknown constant, has negligible spatial variation but is shown to be a function of the DC current density, frequency, ionization coefficients, and the saturated drift velocity. The power transport and the impedance have been calculated from $\overline{E}$ and $\overline{H}$. The quasi-TEM mode is the normal IMPATT mode.

A small discrepancy has been uncovered between the quasi-static results for the normal IMPATT mode diode impedance conventionally used in diode research [Eq. (71)] and the dynamic result [Eq. (76)] developed from multidimensional theory. Fortunately, the magnitude of the numerical discrepancy is negligible for most frequencies of interest except in narrow bands of about 100-MHz width where it may be obscured in practice by other factors. However, the existence of the discrepancy does leave the question of whether its magnitude may not be significant in special diode applications (e.g., at submillimeter frequencies) or for diodes of other types.

The mode spectrum has been determined by the continuity conditions at the planar boundaries $z = \pm L/2$, and the boundary conditions at the planar boundaries $z = +b$ and $z = -a$. This corresponds exactly to the procedure used in the prior one-dimensional theories. As in the theory of radial waveguides, specific conditions at the "rim," i.e., at $r = R$, can be synthesized by an appropriate superposition of avalanche modes assuming mode completeness (which has not been proved here). Generally there are no constraints that may be imposed at $r = R$ because this will vary with the tuning of the associated microwave circuit and particulars of the local structures. An exception is the self-resonant diode.[14]

The spectrum of higher-order modes is discrete and typically involves RF field and RF current profiles which vary strongly with radial position. It is reasonable to expect some coupling between the various avalanche modes to occur as the signal level is increased. Thus, a rigorous large-signal theory of avalanche diodes must evaluate the effects of such mode coupling.

Geometric effects and higher-order modes are considered in detail in the next two parts of this work in Refs. 9 and 14. However, it is useful to describe here, in a qualitative fashion, the

unusual but practical nature of a higher-order mode. Consider an avalanche diode whose cross-sectional area is one to two orders of magnitude greater than those of conventional avalanche diodes operating at the same frequency. The capacitance of such a diode, at microwave frequencies, would be one to two orders of magnitude greater than the permissible level for normal IMPATT operation. However, the preceding observation assumed a uniform RF field profile across the cross section of the diode. If instead the RF field has an exponential taper with radial position, as is approximately true in a SWIMPATT mode, then the effective capacitance would be moderate. Figure 11 illustrates this situation. Further, if one calculates the "effective active volume for the SWIMPATT mode, taking into account the sharp profile, it turns out to be larger for this surface wave than for the corresponding volume wave in normal IMPATT diodes.

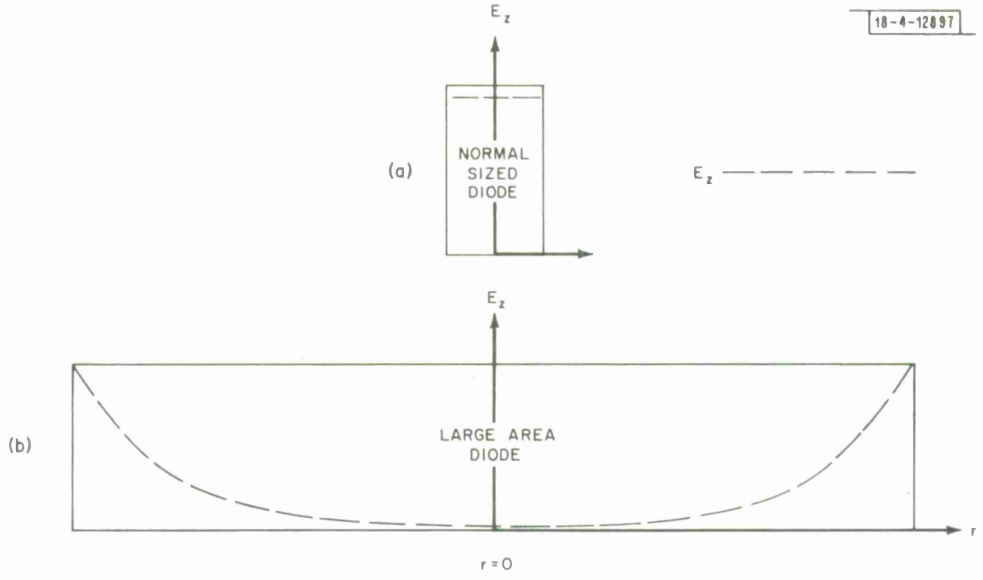

Fig. 11. Radial profiles of axially directed electric field for (a) normal-sized normal IMPATT mode diodes, and (b) large-area SWIMPATT mode diodes.

The buildup of a SWIMPATT wave may be conveniently pictured in two simplified stages. The first stage may occur in a time period of, say, 10 nanoseconds (for an X-band diode) during which the effects of diffusion are too slow to be noticeable. In this stage, the fields and current quickly build up to a state in which they have a steep, nearly exponential variation with radial position, from their peak values at the outer diode perimeter to almost negligible values several tens of microns further inward toward the center of the diode. The power output from such a wave is of the same order as that from the corresponding normal IMPATT diode because the effective active volume of the semiconductor is of the same order in both cases.

As time passes, diffusion occurs because of the steep RF radial gradients in current density. In other circumstances, such diffusion would be small since the carriers would be swept out of the thin active region in the axial direction at their saturated drift speeds (v_s). Their radial excursions would be very limited since their average radial velocities due to diffusion would be very much smaller than v_s. However, avalanching carriers continually produce electron-hole pairs throughout the avalanche zone. Thus, as they travel along their relatively small radial excursions, the avalanching carriers would produce other carriers which would extend the radial excursion and in turn produce other carriers to further extend the radial inflow. The net result

is that the active volume increases markedly so that the output power goes up at least an order of magnitude. However, the inflow of carriers increases the axial electric field further in from the perimeter, which raises the effective capacitance and reduces the frequency of oscillation.

The picture obtained from the above considerations is that of a very large area avalanche diode which produces high power as its frequency of oscillation sweeps over a broad range. Such diodes have been fabricated in the past and their reported operation was considered unexplained in numerous details.[21,22] Now some details may be accurately explained by the above description and by further, more quantitative information to be developed in Ref. 9. For example, calculations based on some normal IMPATT thermal considerations yielded estimates of their sweep frequencies from two to three orders of magnitude off from the observed sweeps, while other more speculative suggestions yield no quantitative estimates.[22] On the other hand, some simple calculations, presented in Ref. 9, obtain both the correct order of magnitude of the sweep frequencies and the correct shape of the curve of sweep frequencies vs time. As a further example, the existence of the SWIMPATT mode and its characteristics explain the descrepancy between Melick's work,[23] (which demonstrated that the RF output IMPATT power peaked for areas around the "normal sized" IMPATT diode and decreased significantly with increasing diode area), and the exceptionally high peak power obtained from the extra large area diodes. These large area diodes produced one to two orders of magnitude more RF power than the normal sized IMPATT diodes (operated at about the same frequency) fabricated by the same workers at their time of discovery.[24] The multiplicity of pulsed modes experimentally detected at the same time and in the same diode by Manasse and Shapiro[25] is also consistent with the multiple mode theory developed in this report and Ref. 9.

A final example is the efficiency predictions of DeLoach based on skin effects in the diode substrate which indicate a marked decrease from the normal efficiency of an IMPATT diode as its radius exceeds the skin depth in the diode substrate.[26] Gilden and Moroney[24] obtained approximately the same efficiencies (5 percent) for 36-mil-diameter diodes as those obtained for normal (4-mil) IMPATT diodes by the same workers at that time. This apparent inconsistency is explainable by the surface-wave character of the SWIMPATT mode.

AKNOWLEDGMENT

The author wishes to thank C. Durney for making available his unpublished analysis on multidimensional avalanche diode theory and his helpful comments. The author is also indebted to R. Sasiela for his comments on an earlier draft of this report. Portions of this work were carried out in conjunction with efforts by R. I. Harrison of New York University and S. P. Denker of the Schumberger-Doll Research Center.

REFERENCES

1. W.J. Read, Jr., "A Proposed High-Frequency, Negative-Resistance Diode," Bell System Tech. J. 37, 401-446 (1958).
2. C. Durney has analyzed a multidimensional solid avalanche diode model in an unpublished memorandum. His formulation, results, and conclusions differ in many respects from those in the present report.
3. H. Berger, "The Mode Spectrum of Avalanche Diodes," Technical Note 1969-31, Lincoln Laboratory, M.I.T. (3 June 1969), DDC AD-690996.
4. W.J. Getsinger, "The Packaged and Mounted Diode as a Microwave Circuit," IEEE Trans. Microwave Theory and Techniques MTT-14, 58-69 (1966).
5. H. Berger, R.I. Harrison, and S.P. Denker, "A New Theory for Carrier-Field Interactions and Electromagnetic Radiation in High-Frequency Avalanche Devices," Solid-State Device Research Conference, Boulder, Colorado (17 June 1968).
6. L.P. Marinaccio, "Ring-Geometry IMPATT Oscillator Diodes," Proc. IEEE 56, 1588-1589 (1967).
7. R.H. Haitz, "Nonuniform Thermal Conductance in Avalanche Microwave Circuit," IEEE Trans. Electron Devices ED-15, 350-361 (1968).
8. D.L. Rode, "Self-Resonant LSA Oscillator Diode," Proc. IEEE 57, 1216-1217 (1969); "Dielectric Loaded Self-Resonant LSA Diode," IEEE Trans. Electron Devices ED-17, 47-52 (1970).
9. H. Berger, "SWIMPATT – A New Microwave Frequency High-Power Avalanche Diode Mode," to be published.
10. H. Sigmund, "Photoelectric Properties of Spherical Avalanche Diodes in Silicon," Infrared Physics 8, No. 4, 259-264 (1968).
11. S. Katoka, H. Tateno, and Mikawashima, "Suppression of Traveling High-Field-Domain Mode Oscillations in GaAs by Dielectric Surface Landing," Elec. Lett. 5, No. 3, 48-90 (6 February 1969).
12. G.S. Kino and P.N. Robson, "The Effect of Small Transverse Dimensions on the Operation of Gunn Devices," Proc. IEEE 56, No. 11, 2056-2057 (1968).
13. K. Kumbe, "Suppression of Gunn Oscillations by a Two-Dimensional Effect," Proc. IEEE 56, No. 12, 2172-2173 (1968).
14. H. Berger, "Complex Geometric Effects in Avalanche Diodes," to be published.
15. H. Berger, "The Influence of Radial Variations of Temperature and Current Density on Avalanche Diode Performance," to be published.
16. T. Misawa, "Multiple Uniform Layer Approximation in Analysis of Negative Resistance in p-n Junctions in Breakdown," IEEE Trans. Electron Devices ED-14, 795-808 (1967).
17. N. Marcuritz, Waveguide Handbook (McGraw-Hill, New York, 1951), pp. 89-96.
18. W.H. Louisell, Coupled Mode and Parametric Electronics (Wiley, New York, 1960), Appendix B.
19. M. Gilden and M.E. Hines, "Electronic Tuning Effects in the Read Microwave Avalanche Diode," IEEE Trans. Electron Devices ED-13, 169-175 (1966).

20. H. Berger, "Negative Conductivity in Solid State Avalanche Diodes," Technical Note 1969-59, Lincoln Laboratory, M.I.T. (16 December 1969), DDC AD-701395.

21. M. Gilden, private communication.

22. C. Buntschuh and M. Gilden, "Integrated Solid-State K_V-band Source," Interim Technical Report No. 2, Microwave Associates, Inc., Air Force Contract No. F33615-67-C-1711 (November 1968).

23. D.R. Melick, "High-Efficiency Pulsed GaAs Avalanche Diodes," Proc. IEEE 55, 435-436 (1967).

24. M. Gilden and W. Moroney, "High Power Pulsed Avalanche Diode Oscillators for Microwave Frequency," Proc. IEEE 55, 1227 (1967).

25. F.K. Manasse and J.S. Shapiro, "Current Dependent Modes in Pulsed Avalanche Diodes," Proc. IEEE 55, 702-703 (1967).

26. B.C. DeLoach, Jr., "Thin Skin IMPATTS," IEEE Trans. Microwave Theory and Techniques, MTT-18, 72-74 (1970).

DOCUMENT CONTROL DATA – R&D

(Security classification of title, body of abstract and indexing annotation must be entered when the overall report is classified)

1. ORIGINATING ACTIVITY *(Corporate author)*
Lincoln Laboratory, M.I.T.

2a. REPORT SECURITY CLASSIFICATION
Unclassified

2b. GROUP
None

3. REPORT TITLE
A Theory of Multiple Modes in Avalanche Diodes

4. DESCRIPTIVE NOTES *(Type of report and inclusive dates)*
Technical Note

5. AUTHOR(S) *(Last name, first name, initial)*
Berger, Henry

6. REPORT DATE	7a. TOTAL NO. OF PAGES	7b. NO. OF REFS
9 June 1970	26	26

8a. CONTRACT OR GRANT NO. AF 19(628)-5167

b. PROJECT NO. 649L

c.

d.

9a. ORIGINATOR'S REPORT NUMBER(S)
Technical Note 1970-17

9b. OTHER REPORT NO(S) *(Any other numbers that may be assigned this report)*
ESD-TR-70-177

10. AVAILABILITY/LIMITATION NOTICES
This document has been approved for public release and sale; its distribution is unlimited.

11. SUPPLEMENTARY NOTES
None

12. SPONSORING MILITARY ACTIVITY
Air Force Systems Command, USAF

13. ABSTRACT

This report develops a multidimensional, dynamic analysis of solid state avalanche diodes. Well-established electromagnetic concepts are applied to a widely used model of the diode and reveal a discrete spectrum of new small-signal modes. The approach used enlarges the conventional perspective and has permitted the discovery that at least one of these new modes appears to possess a high power capability (associated with its two-terminal negative resistance) which has been partially realized experimentally. The lowest-order mode contains all the results of prior quasi-static theories on the normal IMPATT mode, plus additional information which is used to delineate the range of validity of the quasi-static results. Formal discrepancies are uncovered between the usual quasi-static, one-dimensional result for diode impedance used in solid state studies and the dynamic multidimensional result for the normal IMPATT mode developed from microwave circuit theory. However, these discrepancies are numerically quite small except in certain narrow frequency bands.

14. KEY WORDS

avalanche diodes
IMPATT
multiple modes
negative resistance
impedance
high power